

<sup>1</sup>I. E. Dzyaloshinskiĭ, Zh. Eksp. Teor. Fiz. 32, 1547 (1957) [Sov. Phys. JETP 5, 1259 (1957)].  
<sup>2</sup>I. S. Jacobs, R. A. Beyerlein, S. Foner, and J. P. Remeika, Intern. J. Magnetism 1, 193 (1971).  
<sup>3</sup>J. O. Artman, J. C. Murphy, and S. Foner, Phys. Rev. A 138, A912 (1965).  
<sup>4</sup>L. S. Kornienko and A. M. Prokhorov, Zh. Eksp. Teor. Fiz. 33, 805 (1957) [Sov. Phys. JETP 6, 620 (1958)].  
<sup>5</sup>G. S. Bogle and H. F. Symmons, Proc. Phys. Soc. London 73, 531 (1959).  
<sup>6</sup>L. V. Velikov and E. G. Rudashevskii, Zh. Eksp. Teor. Fiz. 56, 1557 (1969) [Sov. Phys. JETP 29, 836 (1969)].  
<sup>7</sup>S. V. Mironov, V. I. Ozhogin, E. G. Rudashevskii, and V. G. Shapiro, Pis'ma Zh. Eksp. Teor. Fiz. 7, 419 (1968) [JETP

Lett. 7, 329 (1968)].  
<sup>8</sup>E. G. Rudashevsky, A. S. Prochorov, and L. V. Velikov, IEEE Trans. Microwave Theory Tech. MTT-22, 1064 (1974).  
<sup>9</sup>S. Foner and S. J. Williamson, J. Appl. Phys. 36, 1154 (1965).  
<sup>10</sup>P. R. Ellison and G. J. Troup, J. Phys. C 1, 169 (1968).  
<sup>11</sup>O. Nagi, N. L. Bonavito, and T. Tanaka, J. Phys. C 8, 176 (1975).  
<sup>12</sup>S. Roberts and I. S. Jacobs, Proc. of Eighteenth Ann. Conf. MMM, Denver, Colorado, 1972, p. 107.  
<sup>13</sup>P. J. Flanders and W. J. Schuele, Proc. Intern. Conf. on Magnetism, Nottingham, 1964, p. 594.

Translated by J. G. Adashko

## Spectral density of parametrically excited waves

I. V. Krutsenko, V. S. L'vov, and G. A. Melkov

Kiev State University

(Submitted 21 April 1978)

Zh. Eksp. Teor. Fiz. 75, 1114-1131 (September 1978)

The spectral density of spin waves excited in ferrites in first-order parametric instability is investigated theoretically and experimentally. It turns out that simultaneous excitation of a large number of degrees of freedom can produce in each individual spin wave appreciable fluctuations (of the order of the amplitude itself) that lead to a substantial nonmonochromaticity of the parametrically excited spin waves. For the case investigated here (single-crystal samples of yttrium iron garnet, room temperature, pump frequency 9.37 GHz), the width of the spectral density of the parametrically excited spin waves is of the order of several kilohertz (at a wave damping decrement of several hundred kilohertz) and depends on the spin-wave damping parameter, on the spin wave vector, and on the supercriticality. The experimental relations are satisfactorily described by the nonlinear theory developed in the paper for parametric excitation of waves in media with a non-decaying dispersion law; these media can be either ferrites or many other physical objects.

PACS numbers: 75.30.Ds, 75.50.Gg

### INTRODUCTION

Parametric excitation is the simplest method of generating waves of high amplitudes with wave vector  $\mathbf{k} \neq 0$  in a solid. However, even in the first experiments on single-crystal ferrites it was noted that the oscillations of parametrically excited spin waves (PSW) are not monochromatic—their frequencies are distributed in a certain interval  $\Delta\omega$  about  $\omega_p/2$ , where  $\omega_p$  is the frequency of microwave magnetic pumping field. This has led to an increase of the noise temperature of the nondegenerate magnetostatic ferrite amplifier<sup>[1]</sup> and to parasitic modulation of the amplitude at the output of ferrite limiters.<sup>[2]</sup> These examples show that information on the frequency distribution of the PSW is quite essential for the design of ferrite devices in which spin waves are parametrically excited.

The presently existing nonlinear theory of parametric wave excitation<sup>[3,4]</sup> does not explain the observed phenomena and calls therefore for further development, all the more since effects that are analogous in many respects to parametric processes in ferrites have been observed and are presently studied in plasma, in ferro-

electrics, in antiferromagnets, and in other nonlinear media.

We have investigated experimentally and theoretically the PSW frequency distribution  $N(\omega)$ :

$$N(\omega) = \int n_{\mathbf{k}\omega} d\mathbf{k},$$

$$\langle a_{\mathbf{k}\omega} a_{\mathbf{k}'\omega'} \rangle = n_{\mathbf{k}\omega} \delta(\mathbf{k}-\mathbf{k}') \delta(\omega-\omega'),$$

$$\langle a_{\mathbf{k}\omega} a_{\mathbf{k}'\omega'} \rangle = \sigma_{\mathbf{k}\omega} \delta(\mathbf{k}+\mathbf{k}') \delta(\omega+\omega'-\omega_p); \quad (1)$$

here  $a_{\mathbf{k}\omega}$  is the Fourier component of the complex amplitude  $a_{\mathbf{k}}(t)$  of a spin wave with wave vector  $\mathbf{k}$ .

The procedure for the measurement of  $N(\omega)$  and the experimental results are presented in Sec. 1. The measurements were made by the parallel-pumping method at a frequency  $\omega_p = 2\pi \cdot 9.37$  GHz on single-crystal yttrium iron garnet (YIG) spheres having a PSW relaxation frequency  $\gamma_{\mathbf{k}} = g\Delta H_{\mathbf{k}}/2 \approx 1$  MHz. It was established that even in the absence of self-oscillations of the magnetization the width  $\Delta\omega$  of the frequency spectrum  $N(\omega)$  is of the order of several kilohertz and depends on the supercriticality, on the values of the PSW wave vectors, and on the parameter  $\Delta H_{\mathbf{k}}$ . The observed

frequency dependence of  $N(\omega)$  is due mainly to fluctuations of the amplitude, whose value is large and of the order of the average amplitude.

There is no doubt that any real parameter has a finite width of the spectrum of the generated frequencies, but the figures given above offer evidence that a ferrite spin-wave generator is much less monochromatic than any other microwave generator. Thus, at a frequency that differs from the central one by 1 kHz the output power of a klystron generator or of a hot-electron generator decreases by more than 10 orders of magnitude,<sup>[5]</sup> whereas  $N(\omega)$  in our experiments decreases in this case by approximately 10%. The situation investigated by us differs in that a large number  $N$  of degrees of freedom (PSW with different  $\mathbf{k}$ ) are simultaneously excited, and this leads to a self-consistent decrease of the effective pump field  $P_h$  to the threshold level  $\gamma_h$  (Ref. 3):

$$hV_{\mathbf{k}} \rightarrow P_{\mathbf{k}} = hV_{\mathbf{k}} + \int S_{\mathbf{k}\mathbf{k}'} n_{\mathbf{k}'} \exp[-i(\varphi_{\mathbf{k}'} - \varphi_{-\mathbf{k}'})] d\mathbf{k}'$$

( $V_{\mathbf{k}}$  and  $S_{\mathbf{k}\mathbf{k}'}$  are the coefficients of the Hamiltonian (22)–(24) below, and  $\varphi_{\mathbf{k}}$  are the phase shifts of the individual waves).

It is seen that  $P_h$  is determined by the total number  $\bar{N}$  of all the PSW, and a change in the amplitude of one of them does not affect significantly the self-consistent field  $P_h$ , making possible giant fluctuation of the amplitudes of individual PSW. The value of  $P_h$  hardly fluctuates in this case:  $\langle \Delta P_h^2 \rangle \approx \bar{N}^{-1} \langle P_h \rangle^2$ .

The large  $\Delta\omega$  of PSW is also due to the fact that  $N$  is large. In fact, in this case the amplitudes of the individual PSW are small, since the energy of the PSW system is distributed over a large number of degrees of freedom  $N$ . This means that a parametric spin-wave is a parametric noise amplifier with not too large a power gain  $K_p$  ( $K_p \sim 10^2 - 10^4$ ) (see Sec. 2). Recognizing that  $\Delta\omega K_p^{1/2} \approx \gamma$  for parametric amplifiers, we obtain the correct order of magnitude of  $\Delta\omega$ .

For a rigorous theoretical determination of the spectrum  $n_{\mathbf{k}\omega}$  it is necessary to go beyond the scope of the self-consistent-field approximation (the S theory). This is done in Sec. 2, where a diagram technique is used to obtain Eqs. (25)–(28) for  $n_{\mathbf{k}\omega}$  and  $\sigma_{\mathbf{k}\omega}$ —the normal and anomalous pair correlators defined by relation (1). These equations have a “one-particle” solution:

$$n_{\mathbf{k}\omega} = n_{\mathbf{k}} \delta(\omega - \omega_p/2), \quad \sigma_{\mathbf{k}\omega} = \sigma_{\mathbf{k}} \delta(\omega - \omega_p/2), \quad (2)$$

which has been analyzed in detail in Ref. 4. We shall show in Secs. 3 and 4 that these equations have also a solution that is regular in  $\omega$ , determine the line widths and shapes of the  $\omega$ -distributions of  $n_{\mathbf{k}\omega}$  and  $\sigma_{\mathbf{k}\omega}$ , and compare the results with experiment in Sec. 5.

There are two causes of the broadening of the spectrum  $n_{\mathbf{k}\omega}$ : thermal noise, which can be described by a Langevin random force, and the “intrinsic” noise due to the interaction of the PSW with one another and described by the off-diagonal terms of the Hamiltonian  $\mathcal{H}_{\text{int}}$ . The scattering of PSW by static inhomogeneities (two-magnon scattering) changes the state of the PSW system and increases the spectral width  $\Delta\omega$  due to the

thermal and intrinsic noise. By itself, however, this scattering does not lead to spectrum broadening, since it proceeds with conservation of the spin wave.

In Sec. 3 we consider the case easiest to analyze theoretically, that of ferromagnets with large concentrations of static inhomogeneities, when the two-magnon damping  $\gamma_{\text{imp}}$  exceeds the intrinsic damping  $\gamma$ . At small supercriticalities the broadening of the spectrum  $n_{\mathbf{k}\omega}$  is due to thermal noise; the  $N(\omega)$  lines are Lorentzians with a width  $\Delta\omega = \eta_p$ :

$$\eta_p \approx \xi \gamma_{\text{imp}} (P-1)^{-1/2}. \quad (3)$$

Here  $\xi$  is a small parameter that characterizes the influence of the thermal fluctuations. For ferromagnets we have<sup>[3]</sup>

$$\xi \approx (\lambda l) (T/T_c) \approx 10^{-2} - 10^{-3}, \quad (4)$$

where  $\lambda$  is the lattice constant,  $\mathbf{k}$  is the PSW wave vector,  $T$  is the temperature,  $T_c$  is the Curie temperature, and  $P = h^2/h_{\text{cr}}^2$  characterizes the excess of the pump power  $h^2$  over the threshold value  $h_{\text{cr}}^2$ .

With increasing supercriticality, the role of the intrinsic noise increases and becomes predominant at  $P > P_1$ , where

$$P_1 - 1 \approx \xi \frac{\gamma}{\gamma_{\text{imp}}} \left( \frac{kv}{\gamma} \right)^{1/2}, \quad (5)$$

( $v = \partial\omega_{\mathbf{k}}/\partial k$  is the group velocity of the PSW). At supercriticalities  $P > P_1$  the  $N(\omega)$  line shape is unusual:

$$N(\omega) = N/\text{ch} \left( \frac{2\omega - \omega_p}{2\eta} \right). \quad (6)$$

The effective line width  $\eta$  increases with increasing supercriticality like

$$\eta \approx \eta_{\text{int}} = \frac{\gamma_{\text{imp}}^2}{\gamma} \left( \frac{\gamma}{kv} \right)^{1/2} (P-1)^{1/2}. \quad (7)$$

These expressions are valid so long as it is possible to disregard vertex renormalization in the diagram series, i.e., at  $P < P_s$  (Ref. 4), where

$$P_s \approx kv/\gamma. \quad (8)$$

Next, in Sec. 4, we study a more complicated case, but more frequently encountered in experiment, case of almost homogeneous ferromagnets:  $\gamma_{\text{imp}} \ll \gamma$ . For the sake of argument we have confined ourselves to the axially symmetrical situation, which is realized in cubic and isotropic ferromagnets (e.g., in YIG) magnetized along the [111] or [100] axis. It is known that the most strongly connected with the pump are PSW propagating across the magnetization ( $\theta_{\mathbf{k}} = \pi/2$ ); these are the only waves excited in the S-theory approximation,<sup>[3]</sup> up to supercriticalities 6–10 dB above threshold. In the near-threshold region (at  $\gamma_{\text{imp}} \ll \gamma$ ), the two-magnon scattering is negligible, and the broadening of the spectrum with respect to  $\theta_{\mathbf{k}}$  and  $\omega$  is connected with the thermal noise:

$$\Delta\theta_{\mathbf{k}} \approx (\eta_p/\gamma)^{1/2}, \quad (9)$$

$$\Delta\omega \approx \eta_p = \gamma \exp[-(P-1)^{1/2}/\xi]. \quad (10)$$

At  $P = P_0$ , where  $P_0$  is given by

$$(P_0 - 1)^{1/2} \approx \xi \ln(\gamma/\gamma_{\text{imp}}),$$

the width  $\Delta\theta_{\mathbf{k}}$  decreases to a value

$$\Delta\theta_{\mathbf{k}} \approx (\gamma_{\text{imp}}/\gamma)^{1/2}, \quad (11)$$

determined by two-magnon scattering, and does not decrease further with increasing supercriticality. At  $P > P_0$  the lines has a Lorentz shape with width  $\Delta\omega \approx \eta_T$ , where

$$\eta_T = \pi \xi \gamma_{imp} / (P-1)^{1/2}. \quad (12)$$

In the absence of two-magnon scattering we can obtain for  $\Delta\omega$  in place of (12) the expression (10), i.e.,  $\eta_T$  has an exponential rather than power-law smallness in terms of the temperature parameter  $\xi$ . Thus, even small two-magnon scattering increases substantially the width of the spectrum. At larger supercriticalities at  $P > P_1$  (but  $P < P_2$ ), where

$$P_1 - 1 \approx \xi P_s (\gamma_{imp}/\gamma)^{1/2}, \quad P_2 - 1 \approx P_s (\gamma_{imp}/\gamma)^{1/2}, \quad (13)$$

the angle broadening is determined as before by the two-magnon scattering,  $\Delta\theta_k$  is determined by formula (9), and the  $\omega$ -broadening is determined by the intrinsic noise. The shape of the  $N(\omega)$  line is close to (6), with an effective width  $\eta = \eta_{intr}$  where

$$\eta_{intr} = \gamma \left( \frac{\gamma_{imp}}{\gamma} \right)^{1/2} \left( \frac{P-1}{P_s} \right)^{1/2}. \quad (14)$$

At larger supercriticalities ( $P > P_2$ ) we can neglect both the thermal fluctuations and the two-magnon scattering. Then

$$\Delta\theta_k \approx (\eta_{intr}/\gamma)^{1/2}, \quad \Delta\omega \approx \eta_{intr}, \quad \eta_{intr} \approx \gamma \left( \frac{P-1}{P_s} \right)^{1/2}. \quad (15)$$

The shape (54) of the  $N(\omega)$  line remains as before close to (6). At the limit of applicability of the theory (at  $P \approx P_s$ ) we have  $\Delta\theta_k \approx \pi$ . Incidentally, supercriticalities of this order are only of academic interest, since self-oscillations set in long before they are reached, and lead to a strong broadening of the spectrum in terms of  $\Delta\theta_k$  and  $\Delta\omega$ .

## 1. EXPERIMENT

For an experimental investigation of the statistical properties of the PSW, we registered electromagnetic radiation from the ferrite at frequencies close to half the pump frequency.<sup>[1,6]</sup> It was shown in Ref. 7 that this phenomenon is due to two-magnon scattering of PSW by statistical inhomogeneities. In this case we can write for the complex amplitude  $U(t)$  of the electromagnetic wave radiated from the crystal

$$U(t) = \sum_{\mathbf{n}} \int g_{\mathbf{k}} \exp(i\mathbf{k}r_{\mathbf{n}}) a_{\mathbf{k}}(t) d\mathbf{k}, \quad (16)$$

where  $g_{\mathbf{k}}$  is the coefficient of transformation of a PSW with wave vector  $\mathbf{k}$  by one scattering center, and  $r_{\mathbf{n}}$  are the coordinates of the center. Using (16), we obtain the correlation function  $K_r(\tau)$  of the radiation:

$$K_r(\tau) = \langle U(t) U^*(t+\tau) \rangle = N_s \int |g_{\mathbf{k}}|^2 n_{\mathbf{k}}(\tau) d\mathbf{k}, \quad (17)$$

where

$$\langle a_{\mathbf{k}}(t) a_{\mathbf{k}'}^*(t+\tau) \rangle = n_{\mathbf{k}}(\tau) \delta(\mathbf{k}-\mathbf{k}')$$

and  $N_s$  is the number of scattering centers.

It is seen from (17) that, apart from a time-independent scale factor, the function  $K_r(\tau)$  is equal to the PSW correlation function integrated with respect to  $\mathbf{k}$

$$N(\tau) = \int n_{\mathbf{k}}(\tau) d\mathbf{k}$$

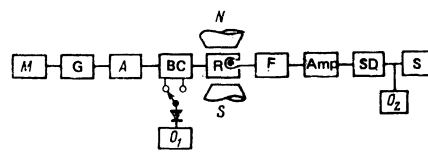


FIG. 1. Block diagram of the experimental setup:  $M$ —magnetron,  $G$ —gate,  $A$ —attenuator,  $BC$ —bidirectional coupler,  $O_1$ ,  $O_2$ —oscilloscopes,  $R$ —resonator with ferrite,  $F$ —low-pass filter,  $Amp$ —amplifier,  $SD$ —square-law detector,  $S$ —spectrum analyzer.

and therefore the spectral density  $K_r(\omega)$  differs only by a constant factor from the PSW spectral density  $N(\omega)$  given by (1). This conclusion stems essentially from the fact that two-magnon scattering by statistical inhomogeneities takes place without a change of the oscillation frequency. It is thus possible to investigate the statistical properties of PSW by studying the electromagnetic radiation from the ferrite.

A block diagram of the experimental setup is shown in Fig. 1. The signal from the magnetron pump generator was fed through a number of waveguide elements to a cavity resonator with a ferrite, located in a constant magnetic field of intensity  $H_0$ . The magnetron operated in the cw regime at 9.37 GHz, and the bandwidth of the magnetron generation did not exceed several hertz. The cavity resonator was a segment of standard rectangular waveguide for the 3-cm band, on one end of which was located an inductive diaphragm for coupling with the pump channel, and the other a metallic wall near which (at a distance 1 mm) was placed the investigated ferrite sphere. The latter was placed inside the coupling loop used to direct the ferrite electromagnetic radiation, of frequency  $\omega_p/2$ , was directed to the recording system. The resonator  $Q$  was  $\sim 500$ , and the oscillation mode  $H_{012}$ . When the spin waves were excited by the parallel-pumping method the plane of the loop and the vectors of the constant and alternating magnetic fields at the location of the ferrite were parallel to one another.

The recording system consisted of a 6-cm-band amplifier guarded against the pump frequency by a low-pulse filter, of a square-law detector, and of a spectrum analyzer and an oscilloscope, on the screens of which it was possible to observe the frequency and temporal characteristics of the radiation from the ferrite. The spectrum analyzers were the instruments SKCh-3 (up to 20 kHz, resolution up to 10 Hz) and Sch-8 (range 20 kHz–3 MHz, resolution 3 kHz).

The investigation objects were ferrite single-crystal YIG spheres of 2.5–2.9 diameter at room temperature. The spheres were oriented with the difficult-magnetization axis [100] parallel to  $H_0$  to exclude the influence of the low-frequency self-oscillations of the magnetization. The electromagnetic radiation from the ferrite was maximal when the frequency of this radiation was equal to the natural frequency of one of the magnetostatic modes. In our case the radiation took place via the modes [220] and [330], which were 20 and 60 Oe lower than the field  $H_c$  at which the PSW with  $\mathbf{k} \rightarrow 0$  were excited. The wave vector of the PSW was varied by changing the constant magnetic field  $H_0$  and was related

in simple fashion to the difference  $\Delta H_c = H_c - H_0$ ;  $k^2 = \Delta H_c/D$ , where  $D$  is the exchange constant. The ferrite spheres were ground with diamond paste of  $\sim 60 \mu\text{m}$  grain, a procedure accompanied by a broadening of the line of homogeneous resonance and magnetostatic modes to 10–20 Oe, as a result of which the electromagnetic radiation could be observed in a wide region near the resonant field of the magnetostatic mode.

Since the recording system contains a square-law detector, the statistical properties of the signal fed to the spectrum analyzer and oscilloscope differ from the statistical properties of the electromagnetic radiation from the ferrite. In fact,<sup>[8]</sup> if the output signal  $U(t) = A(t) \exp(-i\omega_p t/2)$  is narrow-band ( $A(t)$  is a slow function), then the output of the quadratic detector acquires a low-frequency component  $|A(t)|^2 = B(t)$ , as well as a component at the pump frequency  $\omega_p$ . When we use low-pass filters to cut off the signal at the frequency  $\omega_p$ , we lose information concerning the phase, and we investigate within the framework of this procedure the fluctuations of the square of the amplitude of the electromagnetic radiation. The function registered on the screen of the spectrum analyzer is  $I(\Omega) = K_B^{1/2}(\Omega)$ , where

$$K_B(\Omega) = \int K_B(\tau) e^{i\Omega\tau} d\tau = \int \langle B(t)B(t+\tau) \rangle e^{i\Omega\tau} d\tau. \quad (18)$$

If, for example, we use the line (6) as  $N(\omega)$ , then (at  $\Omega \neq 0$ )

$$K_B(\Omega) \propto \int \frac{e^{i\Omega\tau} d\tau}{\text{ch}^2(\pi\eta\tau/2)} = \frac{2\Omega}{\pi\eta^2 \text{sh}(\Omega/\eta)}.$$

The spectrum analyzer should therefore display the relation

$$I(\Omega) \propto \left( \frac{\Omega}{\eta \text{sh}(\Omega/\eta)} \right)^{1/2}. \quad (19)$$

Thus, the spectrum

$$N(\omega) = \text{ch}^{-1} \frac{2\omega - \omega_p}{2\eta}$$

is transformed by the square-law detector in the analyzer into the spectrum (19).

We note that these two functions are very similar to each other if  $\omega_p = 0$  and  $\Omega = \sqrt{6}\omega$ ; the functions

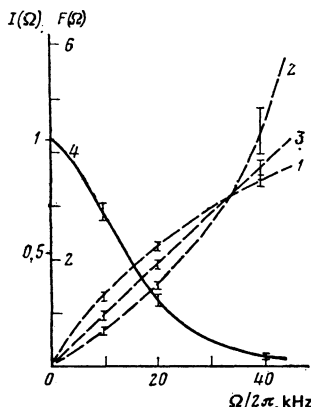


FIG. 2. Spectral density of signal  $I$  passing through the square-law detector vs. the frequency  $\Omega$  for the case of a ferrite single-crystal YLG sphere (2.9 mm diam,  $\Delta H_k = 0.15$  Oe,  $P = 6$  dB)—solid line. Dashed curves—plots of  $I(\Omega)$  in the following coordinates: 1)  $F(\Omega) = 2[\ln[1/I(\Omega)]]^{1/2}$ , 2)  $F(\Omega) = [1/I(\Omega) - 1]^{1/2}$ , 3)  $F(\Omega) = \ln\{1/I(\Omega) + [1/I^2(\Omega) - 1]^{1/2}\}$ .

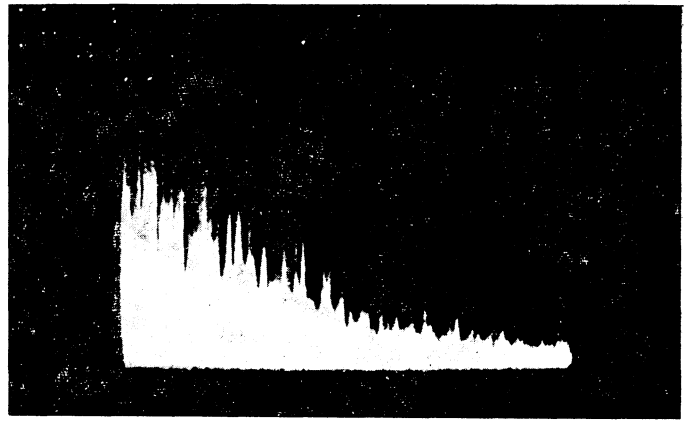


FIG. 3. Photograph of one random realization of the frequency dependence of the spectral density  $I(\Omega)$ . The horizontal sweep is linear with a maximum value 20 kHz.

$(x/\text{sinh } x)^{1/2}$  and  $\text{cosh}^{-1}(x/\sqrt{6})$  are equal accurate to 2.5% at  $|x| \leq 7.3$ ; in this interval both functions change by one order of magnitude. Consequently, the line observed on the spectrum analyzer screen represents, with high accuracy (2.5%), the real electromagnetic radiation, but is broadened by  $\sqrt{6}$  times.

Figure 2 shows a typical experimental plot of  $I(\Omega)$  for one of the investigated YIG spheres. The solid curve in Fig. 2 is a smoothed curve based on ten realization of the random process on the spectrum-analyzer screen. A photograph of one of the realizations is shown in Fig. 3.

To clarify the character of the experimental  $I(\Omega)$  curve, it was plotted in three sets of rectifying coordinates:  $[\ln(1/I)]^{1/2}$ ,  $\Omega$ ;  $(1/I - 1)^{1/2}$ ,  $\Omega$  and  $\ln[1/I + (1/I^2 - 1)^{1/2}]$ ,  $\Omega$ . If  $I(\Omega)$  is a Gaussian curve,  $I(\Omega) \sim \exp[-\Omega^2/\Delta\Omega^2]$ , then its plot will be a straight line in the first set of coordinates; if  $I(\Omega)$  is a Lorentzian, then the plot will be straight in the second set; if  $I(\Omega)$  is described by formula (19), then a straight plot of  $I(\Omega)$  will be obtained in the third set of coordinates. It is seen from Fig. 2 that the first two standard functions are not at all suitable for the description of the experiment, whereas the function (19) agrees satisfactorily with the experiment. The same agreement was observed for the shape of the  $I(\Omega)$  curve of all the samples investigated by us at various supercriticalities and various values of the constant magnetic field. The slope of the straight line on Fig. 2 determines the width  $\Delta\Omega$  of the curve; this width, as indicated above, is  $\sqrt{6}$  times larger than the real width  $\Delta\omega$  of the electromagnetic-radiation curve, which coincides with the width of the spectral density of the PSW.

In the course of the experiment we measured the dependences of  $\Delta\Omega$  and  $\eta$  on the quantity  $\Delta H_c = Dk^2$ , on the spin-wave damping parameter  $\Delta H_k = 2\gamma_k/g$ , and on the supercriticality  $P = h^2/h_{cr}^2$ . The results of these measurements are shown in Figs. 4–6 and will be discussed after the exposition, in the sections that follow, of the rigorous theory of parametric excitation of spin waves in ferrites. Figure 7 shows a photograph of a random realization of radiation from a ferrite, taken from the

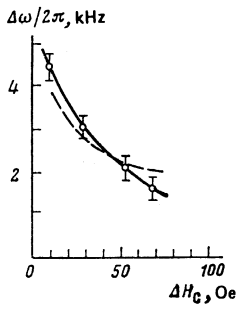


FIG. 4. Dependence of the width  $\Delta\omega$  of the spectral density of the PSW on the constant magnetic field  $\Delta H_c = H_c - H_0$ . Sample—YLG sphere (2.9 mm diam,  $P=1$  dB);  $\Delta H_k = \Delta H_k(\Delta H_c)$ , the points correspond to  $\Delta H_k(10 \text{ Oe})=0.13 \text{ Oe}$ ,  $\Delta H_k(30 \text{ Oe})=0.15 \text{ Oe}$ ,  $\Delta H_k(50 \text{ Oe})=0.155 \text{ Oe}$ , and  $\Delta H_k(70 \text{ Oe})=0.165 \text{ Oe}$ . Dashed—theory (see Sec. 5).

screen of oscilloscope  $O_2$  and representing the time dependence of the square of the radiation amplitude.

As already noted, all the results reported above were obtained with spherical samples under conditions of parallel pumping of the spin-wave instability and at an orientation of  $H_0$  along the difficult magnetization axis [100]. When  $H_0$  deviates from [100] by about  $20^\circ$ , low-frequency self-oscillations of the magnetization appear and broaden substantially the spectrum of the electromagnetic radiation. This broadening is maximal at  $H_0 \parallel [111]$ , when  $\Delta\omega$  exceeds by about two orders of magnitude the corresponding value of  $\Delta\omega$  at  $H_0 \parallel [100]$ . In the case of perpendicular pumping of the spin-wave instability, the situation is reversed: the most monochromatic radiation from the ferrite sphere is observed at  $H_0 \parallel [111]$ , and the parameters of this radiation do not differ in any way from those shown in Figs. 2–6.

We note in conclusion we note that the spectral density of the PSW radiation was measured also in a sample in the form of a disk magnetized perpendicular to its plane (disk diameter 4.5 mm, thickness 1.4 mm). In this case the radiation from the ferrite is due not to random inhomogeneities but the regular gradient of the internal magnetic field,<sup>[9]</sup> and therefore the intensity greatly exceeds (by more than two orders) the intensity of the radiation of spherical samples. In all other respects the data obtained with the disk were perfectly analogous to

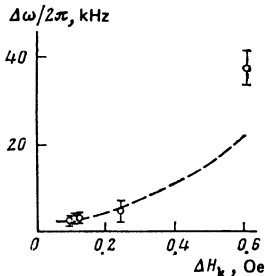


FIG. 5. Dependence of the width  $\Delta\omega$  of the PSW spectral density on the spin-wave damping parameter  $\Delta H_k$  for  $\Delta H_c = 30 \text{ Oe}$  and  $P=1$  dB. The data at  $\Delta H_k = 0.2 \text{ Oe}$  were measured for different single-crystal YLG spheres. The experimental point corresponding to  $\Delta H_k = 0.6 \text{ Oe}$  was measured for a polycrystalline YLG sphere of 2.7 mm diameter. Dashed curve—theory (see Sec. 5).

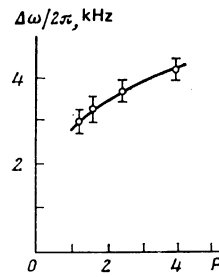


FIG. 6. Dependence of width  $\Delta\omega$  of PSW spectral density of the supercritically  $P=(h/h_{cr})^2$  for a YLG sphere (2.9 mm diam);  $\Delta H_c = 30 \text{ Oe}$ ,  $\Delta H_k = 0.15 \text{ Oe}$ .

the results shown in Figs. 2–6; this is additional evidence that the statistical properties of the radiation do not depend on the mechanism whereby the PSW is converted into an electromagnetic wave, but are determined by the properties of the PSW itself.

## 2. FUNDAMENTAL EQUATIONS OF THE THEORY

As usual, we start with the classical Hamilton's equations of motion for the complex amplitudes  $a_k$  of the traveling waves:

$$i\dot{a}_k = \delta\mathcal{H}/\delta a_k^* \quad (20)$$

The Hamiltonian of the problem

$$\mathcal{H} = \int \omega_k a_k a_k^* dk + H_p + H_{imp} + H_{int} \quad (21)$$

includes the interaction of the waves with the homogeneous pump field  $h(\mathbf{r}, t) = h \exp(-i\omega_p t)$ :

$$\mathcal{H}_p = \frac{1}{2} \int [h(t) V_k a_k a_{-k}^* + \text{c.c.}] dk, \quad (22)$$

the interaction of the waves with the statistical inhomogeneities:

$$\mathcal{H}_{imp} = \int g_{kk'} a_k a_{k'}^* b_{k''} \delta(k - k' - k'') dk dk' dk'' \quad (23)$$

and their interaction  $\mathcal{H}_{int}$  with one another. In the case of a decaying dispersion law, when all the excited waves are concentrated near the surface  $2\omega_k = \omega_p$ , we have

$$\mathcal{H}_{int} = \frac{1}{2} \int T_{12,31} a_1^* a_2^* a_3 \delta(k_1 + k_2 - k_3) dk_1 dk_2 dk_3. \quad (24)$$

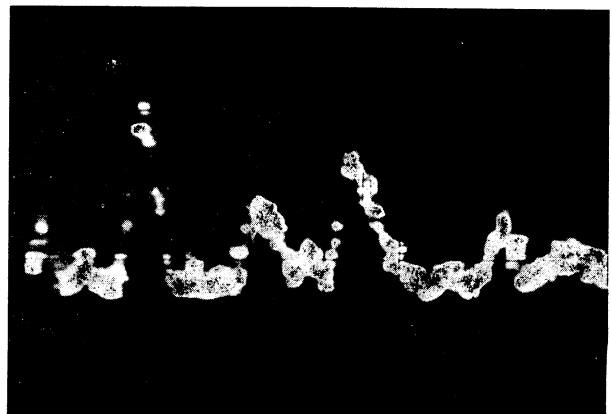


FIG. 7. Photograph of one random realization of the time dependence of the square of the amplitude  $|A(t)|^2$  of radiation from a ferrite. Horizontal sweep duration  $400 \mu \text{ sec}$ .

For a statistical description of parametrically excited waves (PW), one of us<sup>[4]</sup> used a canonical diagram technique<sup>[10]</sup> that generalized the technique developed by Wyld for hydrodynamic-turbulence problems.<sup>[11]</sup> The smallness of the interaction of the PW with one another, relative to their dispersion, allows us to restrict ourselves to partial selective summation of the diagrams of nonrenormalizing vertices. Solving the Dyson equations obtained in this manner,<sup>[4]</sup> we have for the normal and anomalous Green's functions  $G_{\mathbf{k}\omega}$  and  $L_{\mathbf{k}\omega}$

$$\begin{aligned} G_q &= (\omega_p - \omega - \bar{\omega}_k - i\Gamma_q) \Delta_q^{-1}, & L_q &= \Pi_q \Delta_q^{-1}, \\ \Delta_q &= (\omega_p - \omega - \bar{\omega}_k - i\Gamma_q) (\omega - \bar{\omega}_k + i\Gamma_q) - |\Pi_q|^2, & & \\ q &= \mathbf{k}, \omega, \bar{q} = -\mathbf{k}, \omega_p - \omega. \end{aligned} \quad (25)$$

If the pump amplitude is not too large,  $P < P_S$  (see Eq. (7)), we can disregard the diagrams of second order in  $\mathcal{H}_{\text{int}}$  in the expressions for the spin-wave (SW) frequency  $\bar{\omega}_k$ , for the damping  $\Gamma_q$ , and the renormalized pump amplitude  $\Pi_q$ . Then

$$\begin{aligned} \bar{\omega}_k &= \omega_k + 2 \int T_{\mathbf{k}\mathbf{k}'} n_{q'} dq', & \Gamma_q &= \gamma_k - c \int |g_{\mathbf{k}\mathbf{k}'}|^2 \text{Im} G_{\mathbf{k}'\omega} dk', \\ \Pi_q &= P_k + c \int g_{\mathbf{k}\mathbf{k}'} g_{-\mathbf{k}, -\mathbf{k}'} L_{\mathbf{k}'\omega} dk', & & \\ P_k &= \hbar V_k + \int S_{\mathbf{k}\mathbf{k}'} \sigma_{q'} dq', & & \\ T_{\mathbf{k}\mathbf{k}'} &= T_{\mathbf{k}\mathbf{k}', \mathbf{k}\mathbf{k}'}; & S_{\mathbf{k}\mathbf{k}'} &= T_{\mathbf{k}, -\mathbf{k}, \mathbf{k}', -\mathbf{k}'} \end{aligned} \quad (26)$$

Compared with Ref. 4, we take here additional account of the interaction with the random inhomogeneities (of the concentration  $c$ ) and it is not assumed that  $\omega = \omega_p/2$ . In (26),  $\gamma_k$  is the SW damping decrement in a homogeneous crystal in the absence of pumping. This decrement can be calculated with the aid of the kinetic equation.  $n_q$  and  $\sigma_q$  are the normal and anomalous pair correlators (1). It is possible to obtain for them<sup>[4]</sup> closed integral equations that generalize the equations of the S theory:

$$\begin{aligned} n_q &= G_q A_q + L_q B_q^*, & \sigma_q &= G_q A_q^* + L_q B_q, \\ A_q &= \Phi_q G_q^* + \Psi_q L_q^*, & B_q &= \Psi_q G_q + \Phi_q L_q. \end{aligned} \quad (27)$$

Unlike relation (26), in the diagrams for  $\Phi_q$  and  $\Psi_q$  we must take into account terms of second order in  $\mathcal{H}_{\text{int}}$ :

$$\begin{aligned} \Phi_q &= \Phi_{\text{imp}}(q) + \Phi_{\text{int}}(q), & \Psi_q &= \Psi_{\text{imp}}(q) + \Psi_{\text{int}}(q); \\ \Phi_{\text{imp}}(q) &= c \int |g_{\mathbf{k}\mathbf{k}'}|^2 n_{\mathbf{k}'\omega} dk', & \Psi_{\text{imp}}(q) &= \int g_{\mathbf{k}\mathbf{k}'} g_{-\mathbf{k}, -\mathbf{k}'} \sigma_{\mathbf{k}'\omega} dk, \\ \Phi_{\text{int}} &= 2 \int [ |T_{\mathbf{k}_1, 23}|^2 n_1 n_2 n_3 & & \\ &+ T_{\mathbf{k}_1, 23} T_{\mathbf{k}_2, 13} \sigma_1 (n_2 \sigma_3 + \sigma_2 n_3) ] \delta^4(q + q_1 - q_2 - q_3) d^3 q_1 d^3 q_2 d^3 q_3, & & \\ \Psi_{\text{int}} &= 2 \int [ T_{\mathbf{k}_1, 23}^2 \sigma_1^* \sigma_2 \sigma_3 & & \\ &+ T_{\mathbf{k}_1, 23} T_{\mathbf{k}_2, 13} + n_1 (\sigma_2 n_3 + \sigma_3 n_2) ] \delta^4(q + q_1 - q_2 - q_3) d^3 q_1 d^3 q_2 d^3 q_3. \end{aligned} \quad (28)$$

In the next section we consider Eqs. (25)–(28) in the case easiest to analyze theoretically, when the defect concentration is large and the “two-magnon damping”  $\gamma_{\text{imp}} \gg \gamma$ .

### 3. MULTIFREQUENCY TURBULENCE OF SPIN WAVES IN CRYSTALS WITH DEFECTS

It was shown in Ref. 12 that random inhomogeneities destroy the phase correlation in SW and at  $\gamma_{\text{imp}} \gg \gamma$  we have

$$\begin{aligned} |\sigma_k|/n_k &\approx (\gamma/\gamma_{\text{imp}})^{1/2} \ll 1, \\ |P_k|^2 &\approx |\Pi_q|^2 \approx \gamma \gamma_{\text{imp}} \ll \Gamma^2 \approx \gamma_{\text{imp}}^2. \end{aligned}$$

This circumstance allows us to simplify greatly Eqs. (25)–(28), in which retain, besides the principal terms, only the terms of first order in the parameter  $\gamma/\gamma_{\text{imp}}$ . We can neglect in the resultant equations the dependences of  $\Phi_{\mathbf{k}\omega}$  and  $\Psi_{\mathbf{k}\omega}$  on the modulus of  $\mathbf{k}$ , and this enables us to integrate them and obtain closed equations for the integral quantities

$$n_{\omega} = k_{\omega}^2 \int n_{\mathbf{k}\omega} d\mathbf{k}, \quad \sigma_{\omega} = k_{\omega}^2 \int \sigma_{\mathbf{k}\omega} d\mathbf{k}. \quad (29)$$

We have

$$\begin{aligned} \Gamma_{\omega} n_{\omega} &= \frac{\pi k_{\omega}^2}{v} \left\{ \Phi_{\omega} \left[ 1 + \frac{|\Pi_{\omega}|^2 [(\Delta\omega)^2 + 3\Gamma_{\omega}^2]}{2[\Gamma_{\omega}^2 + (\Delta\omega)^2]} + \frac{\text{Re} \Pi_{\omega} \Psi_{\omega}'}{\Delta\omega + i\Gamma_{\omega}} \right] \right\}, \\ \Gamma_{\omega} \sigma_{\omega} + i \Pi_{\omega} n_{\omega} &= 0, \end{aligned} \quad (30)$$

where

$$\begin{aligned} \Gamma_{\omega} &= \gamma_{\omega} + \pi c \int |g_{\omega\omega'}|^2 \frac{k_{\omega'}^2}{v_{\omega'}} \left( 1 + \frac{|\Pi_{\omega'}|^2 [\Gamma_{\omega'}^2 - (\Delta\omega)^2]}{2[\Gamma_{\omega'}^2 + (\Delta\omega)^2]} \right) \\ \Pi_{\omega} &= P_{\omega} + \pi c \int g_{\omega\omega'} g_{\omega\omega'}' \frac{k_{\omega'}^2}{v_{\omega'}} \frac{\Pi_{\omega'} d\Omega'}{\Gamma_{\omega'} - i(\Delta\omega)}. \end{aligned} \quad (31)$$

Here  $\Omega$  is the solid angle of  $\theta$  and  $\varphi$ ;  $\bar{\Omega}$  is that of  $\pi - \theta$  and  $\varphi + \pi$ ;  $d\Omega = d \cos\theta d\varphi$ ;  $\Delta\omega = \omega - \omega_p/2$ .

In the limit  $\gamma_{\text{imp}} \gg \gamma$ , Eqs. (30) and (31) have the isotropic solution  $n_{\omega} = N_{\omega}/4\pi$ . Integrating (30) with respect to  $\Omega$  and taking relations (31) into account, we obtain an equation for the dependence of  $N_{\omega}$  on  $\omega$ :

$$N_{\omega} = \frac{\pi \Gamma_1}{(\eta^2 + \omega^2)} \int \frac{k_{\omega}^2}{v_{\omega}} \Phi_{\text{int}}(\Omega, \omega) d\Omega, \quad (32)$$

where

$$\begin{aligned} \Gamma_1^{-1} &= \frac{\gamma_{\text{imp}}}{g^2} \int \frac{d\Omega d\Omega'}{16\pi^4} \frac{|g_{\omega\omega'}|^2 \text{Re} P_{\omega} \Pi_{\omega'}}{\Gamma_{\omega'}^4}, \\ \gamma_{\text{imp}} &= \frac{4\pi^2 g^2 k^2}{v}, \\ \frac{g^2 k^2}{v} &= \int \frac{k_{\omega}^2 |g_{\omega\omega'}|^2 d\Omega d\Omega'}{v_{\omega} 16\pi^2}. \end{aligned}$$

In order of magnitude we have  $\Gamma_1 \approx \gamma_{\text{imp}}^2/\gamma$ , and the condition  $\eta^2 = 0$  determines the threshold of the parametric excitation of the SW:  $|\hbar V|^2 \approx \gamma \gamma_{\text{imp}}$ . The term  $\Phi_{\text{int}}$  in (28) consists of two parts: a thermodynamic-equilibrium contribution  $\Phi_0 = \gamma n_k^0/\pi$  and a term  $\Phi_3$  that is cubic in the amplitudes  $n_{\omega}$  and for which an expression is obtained from (28) by integrating over the wave vectors. As a result we have

$$\begin{aligned} N_{\omega} &= \frac{\Gamma_1}{\eta^2 + (\Delta\omega)^2} \left[ \frac{4\pi k^2 n_k^0}{v} + \frac{T^2}{kv} \int N_{\omega_1} N_{\omega_2} N_{\omega_3} \delta(\omega + \omega_1 - \omega_2 - \omega_3) d\omega_1 d\omega_2 d\omega_3 \right], \end{aligned} \quad (33)$$

where  $T$  is the mean value of the square of the matrix element  $T_{\mathbf{k}_1, 23}$ . At low spuercriticalities, when the second term in (33) can be neglected, the distribution  $n_{\omega}$  is Lorentzian with width  $\eta = \eta_T$ ; this width can be determined by integrating (33) with respect to:

$$\eta_T = \frac{\Gamma_1 \gamma}{kv} \frac{4\pi^2 k^2 n_k^0}{N} \approx \frac{\gamma_{\text{imp}}}{kv} \frac{4\pi^2 k^2 n_k^0}{N}. \quad (34)$$

Here  $N = \int N_{\omega} d\omega$  is the integral amplitude of the SW. Recognizing that<sup>[13]</sup>

$$TN \approx \gamma_{imp} (P^2 - 1)^{1/2}, \quad P = (h/h_{cr})^2, \quad (35)$$

we obtain for  $\eta_T$  formula (3), in which

$$\xi = 4\pi^2 k^2 T n_k^0 / v. \quad (36)$$

In the opposite case of large supercriticality we can neglect the thermal term in (33) and solve this equation by changing to the  $\tau$ -representation using the formulas

$$N(\tau) = (2\pi)^{-1/2} \int_{-\infty}^{\infty} N(\omega) e^{-i\Delta\omega\tau} d\omega, \quad (37)$$

$$\left[ \frac{d^2}{d\tau^2} - \eta^2 \right] N(\tau) = - \frac{2\pi\Gamma_1 |T|^2}{kv} N^2(\tau).$$

For  $n(\tau)$  we obtained Newton's equation with a "potential energy"

$$\Pi(N) = - \frac{\eta^2 N^2}{2} + \frac{\pi\Gamma_1 T^2 N^3}{2kv}.$$

This equation has an integral of "motion"  $\frac{1}{2}(dN/d\tau)^2 + \Pi = E$ , which makes it possible to integrate it once. The trivial solution of (37), which does not depend on  $\tau$ , corresponds to the "single-particle" solution of (33):  $N(\omega) \propto \delta(\omega - \omega_p/2)$ .

At  $E > \Pi_{\min}$ , a solution  $N(\tau)$  that oscillates with a frequency  $2\eta$  appears, and the expression for  $N(\omega)$  acquires in this case, besides the central line (whose intensity decreases) also satellites whose frequency differ from  $\omega_p/2$  by  $\delta\omega = \pm 2\eta m$  ( $m$  is an integer). With increasing  $E$ , the value of  $\delta\omega$  decreases, the number harmonics, and at  $E = 0$  the solution  $N(\omega)$  becomes a continuous function of  $\omega$ :

$$N(\tau) = \frac{(\pi kv)^{1/2}}{2T\Gamma_1} \frac{\eta}{\text{ch } \eta\tau}, \quad TN(\omega) = \left( \frac{kv}{2\Gamma_1} \right)^{1/2} \text{ch}^{-1} \frac{\pi\omega}{2\eta}. \quad (38)$$

Thus, Eq. (33) has a one-parameter set of solutions corresponding to variation of  $E$  from  $\Pi_{\min}$  to 0. The theoretical choice of the solution, which must be realized in actuality, should be based on a solution of the stability problem within the framework of the total Hamiltonian. Our experiment shows that the distribution  $N(\omega)$  in yttrium garnet is continuous, and this distribution will be investigated.

To estimate its width  $\eta$ , we calculate the central amplitude of the distribution (38):

$$N = \int N(\omega) d\omega = \frac{\pi\eta}{T} \left( \frac{kv}{2\Gamma_1} \right)^{1/2}. \quad (39)$$

Substituting here expressions (32) and (35) for  $\Gamma_1$  and  $N$ , we obtain the estimate (7) for  $\eta$ . The total width consists of the thermal width (3) and the intrinsic width (7). The minimal width  $\eta_{\min}$  is reached at the supercriticality  $P_{\min}$ :

$$\eta_{\min} \approx \gamma_{imp} \left( \xi \frac{\gamma_{imp}}{\gamma} \right)^{1/2} \left( \frac{\gamma}{kv} \right)^{1/4} \approx (0.1-0.01) \gamma_{imp} \left( \frac{\gamma_{imp}}{\gamma} \right)^{1/2}, \quad (40)$$

$$P_{\min}^2 - 1 \approx \xi \frac{\gamma}{\gamma_{imp}} \left( \frac{kv}{\gamma} \right)^{1/2} \approx 0.1 \frac{\gamma}{\gamma_{imp}}. \quad (41)$$

#### 4. MULTIFREQUENCY TURBULENCE IN ALMOST HOMOGENEOUS CRYSTALS

1. *Fundamental equations.* In this section we consider a more complicated case, when the defect concentra-

tion is low, so that  $\gamma_{imp} \ll \gamma$ . The phase correlations in the pairs are large in this case:  $|\sigma_k| \approx n_k$ , it is necessary to study the initial equations (25)-(28). Neglecting the dependence of the matrix elements  $T_{k_1, 23}$  on the moduli  $k_i$  (relative to the parameter  $\gamma/kv \ll 1$ ), we integrate these equation with respect to the modulus  $k$ . As a result we obtain rather cumbersome equations for the quantities  $n_{\omega\Omega}$  and  $\sigma_{\omega\Omega}$ . As we shall show below, at  $\gamma_{imp} \ll \gamma$  the width of the distributions of  $n_{\omega\Omega}$  or  $\sigma_{\omega\Omega}$  with respect to  $\omega$  is much narrower than  $\gamma$ , so that these equations can be simplified by putting  $\Delta\omega = \omega - \omega_p/2 \ll \gamma$ . We have

$$n_{\omega\omega} = \frac{\pi k_{\omega}^2 [\gamma_{\omega} \Phi_{\omega\omega} + \text{Im}(P_{\omega} \Psi_{\omega\omega})]}{2(2\gamma_{\omega})^{1/2} v_{\omega} [(\Delta\omega)^2 + \eta_{\omega}^2]^{3/4}},$$

$$\gamma_{\omega} \sigma_{\omega\omega} + iP_{\omega} n_{\omega\omega} = 0; \quad (42)$$

here

$$\eta_{\omega} = [\gamma_{\omega}^2 - |P_{\omega}|^2] (2\gamma_{\omega})^{-1}$$

and no account was taken (relative to the parameter  $\gamma_{imp} \ll \gamma$ ) of the renormalization of the Green's functions.

In this approximation, the contribution of the defects must be taken into account only in the expressions for  $\Phi_{\Omega\omega}$  and  $\Psi_{\Omega\omega}$ . Confining ourselves to the axially symmetrical case, we assume that the PSW are concentrated on the equator of the resonant surface  $\mathbf{k} \perp \mathbf{M}$ . In this case  $n_{\Omega} = n_{\theta}$  and  $\sigma_{\Omega} = \sigma_{\theta} e^{-2i\varphi}$ , where  $\theta$  is the polar angle and  $\varphi$  is the azimuthal (in the plane  $\mathbf{k} \perp \mathbf{M}$ ) angle;  $P_{\Omega} = P_{\theta} e^{-2i\varphi}$ . We can put  $\eta = 0$  in the numerator of (42), i.e., assume  $|P_{\theta}| = \gamma_{\theta}$  and  $|\sigma_{\theta}| = n_{\theta}$ . Using all this, we simplify (42):

$$n_{\theta\omega} = \left( \frac{\gamma}{2} \right)^{1/2} \frac{\pi}{[(\Delta\omega)^2 + \eta_{\theta}^2]^{3/4}} \left[ \frac{\gamma n_k^2 k^2}{2v} + \frac{2\pi g^2 k^2 c}{v} \int n_{\theta\omega} d\theta + \frac{S^2}{kv} \int n_{\theta\omega} n_{\theta\omega} \right]$$

$$\times n_{\theta\omega} \delta(\theta + \theta_1 - \theta_2 - \theta_3) \delta(\omega + \omega_1 - \omega_2 - \omega_3) \prod_{i=1}^3 d\omega_i d\theta_i. \quad (43)$$

Here

$$g^2 = \frac{1}{2\pi} \int [ |g_{\omega\omega'}|^2 + \text{Im} g_{\omega\omega'}^2 \exp\{2i(\varphi - \varphi')\} ] d\varphi',$$

$$S^2 = \sum_n S_{2n} (S_{2n} - S_{-2n}) \int \delta(\mathbf{a} + \mathbf{a}_1 - \mathbf{a}_2 - \mathbf{a}_3) d\varphi_1 d\varphi_2 d\varphi_3,$$

where  $S_n$  is the Fourier component, with respect to  $\varphi - \varphi'$ , of the coefficients

$$S_{kk'} = S(\varphi - \varphi') \exp\{-2i(\varphi - \varphi')\}$$

of the diagonal part of the Hamiltonian  $\mathcal{H}_{int}$ . The concrete expressions for  $S_{2n}$  are given in the review<sup>[3]</sup> (see formulas (4.3) and (4.5)-(4.9)), and  $\mathbf{a}_i$  are unit vectors in the plane  $\mathbf{k}_i \perp \mathbf{M}$ .

In cubic ferromagnets, the function  $\eta_{\theta}$  is minimal at  $\theta = \pi/2$ ; it can be represented in the form

$$\eta_{\theta} = \eta + 1/2 b \gamma x^2, \quad x = \pi/2 - \theta \ll 1, \quad (44)$$

where the dimensionless coefficient is of the order of unity and depends on the supercriticality  $P$ . As  $P \rightarrow 1$  we have  $b \rightarrow 1$ . Using (26), (42), and (44), we obtain under our assumptions an equation for  $\eta$ :

$$2\gamma\eta = \gamma^2 - |P|^2, \quad \gamma = \gamma(\pi/2), \quad P = P(\pi/2),$$

$$P = hV - 2\pi i S_0 \frac{P}{\gamma} \int n_{\omega\omega} d\theta d\omega. \quad (45)$$

We analyze next the obtained system (43)–(45) in three cases: small, large, and intermediate supercriticality.

2. *Small supercriticality.* In this case we can neglect the last term of (43) and integrate the expression with respect to  $\theta$ . As a result we arrive at a simple equation for  $N_\omega$ :

$$N_\omega = \frac{2\pi \int n_{\omega\theta} d\theta}{v[(\Delta\omega)^2 + \eta^2]^{3/2} - d\gamma_{\text{imp}}}. \quad (46)$$

Here  $d \approx 1$ , and  $\gamma_{\text{imp}} = 4\pi g^2 k^2 c/v$ . At  $n < \gamma$  we can simplify Eqs. (45) to

$$(S_\omega N)^2 = (\hbar V)^2 - \gamma^2 + 2\gamma\eta, \quad (47)$$

$$N = \int N_\omega d\omega = 2\pi \int n_{\omega\theta} d\cos\theta d\omega.$$

At small  $N$  we have  $\gamma_{\text{imp}} < \eta$  and we can put in (46)  $\gamma_{\text{imp}} = 0$  and integrate with respect to  $\omega$ . Together with (47), the result determines the dependence of  $S_\omega N$  and of  $\eta$  on  $\hbar V$ . For example, at  $\hbar V = \gamma$  we have

$$S_\omega N = \xi \gamma \ln \frac{2\gamma^2}{(S_\omega N)^2} \approx 2\gamma \xi |\ln \xi|, \quad (48)$$

$$\eta = \eta_T \approx \gamma \sqrt{\xi}.$$

At  $\hbar V - \gamma > \gamma \xi$  the width  $\eta_T$  is determined by formula (10) and

$$S_\omega N = \gamma (P^2 - 1)^{1/2}. \quad (49)$$

The estimate (10) for  $\eta_T$  at  $\gamma_{\text{imp}} = 0$  was obtained earlier by another method by one of us with Zakharov.<sup>[12]</sup> With increasing supercriticality,  $\eta_T$  at  $\gamma_{\text{imp}}$  and formulas (48) and (10) for  $\eta$  turn out to be incorrect. The decrease of  $\eta$  stops:  $\eta \rightarrow d\gamma_{\text{imp}}$ , and this makes it possible to simplify (46) to

$$N_\omega = \frac{4\pi^2 \gamma \gamma_{\text{imp}} k^2 n_k^0}{v[(\Delta\omega)^2 + \eta^2]^{3/2}} \tilde{\eta}^2 = 2d\gamma_{\text{imp}} (\eta - d\gamma_{\text{imp}}). \quad (50)$$

Integrating (50) with respect to  $\omega$  we obtain the estimate (12) for the thermal width  $\tilde{\eta}_T$  of the distribution (50).

The estimate (12) obtained at  $\gamma_{\text{imp}} \ll \gamma$  agrees with the estimate (3) obtained at  $\gamma_{\text{imp}} \gg \gamma$ , and is thus valid for any ratio of  $\gamma_{\text{imp}}$  and  $\gamma$ . It must only be borne in mind that  $\xi$  in (12) is expressed in terms of  $k^2/v$  on the equator of the resonance surface, whereas in (3)  $k^2/v$  is the averaged quantity

$$\left\langle \frac{k^2}{v} \right\rangle = \int_0^1 k_\theta v_\theta^{-1} d\cos\theta.$$

For the real spectrum of  $\omega_k$  in cubic ferromagnets, these quantities can differ by more than one order of magnitude.

The width of the distribution of  $n_{\theta\omega}$  in  $\theta$  can be determined from (42) and (44) if account is taken of the result  $\gamma \approx \gamma_{\text{imp}}$  that follows from (50); in this case we get the estimate (11).

3. *Region of intermediate supercriticality.* This region corresponds to a situation wherein it is necessary to take into account in Eq. (43) for  $n_{\theta\omega}$  all three terms: the thermal noise  $\propto n_k^0$ , the impurity term  $\propto \gamma_{\text{imp}}$ , and the intrinsic noise  $\propto T^2 N^2$ . Then (43) can not be reduced to

an equation for the integral quantity  $N_\omega$ , but a qualitatively correct result is obtained if, in the integration of (43) with respect to  $\theta$ , we confine ourselves to an estimate of the third term of the distribution  $n_{\theta\omega}$  with effective width  $\Delta\theta$  (11). Proceeding in this manner and assuming that  $\Delta\omega \ll \gamma_{\text{imp}}$ , we obtain in lieu of (50)

$$N_\omega = \frac{\pi \gamma_{\text{imp}}}{(\Delta\omega)^2 + \tilde{\eta}^2} \left[ \frac{4\pi \gamma n_k^0 k^2}{v} + \frac{T^2}{kv\Delta\theta} \int N_{\omega_1} N_{\omega_2} N_{\omega_3} \delta(\omega + \omega_1 - \omega_2 - \omega_3) d\omega_1 d\omega_2 d\omega_3 \right].$$

This equation is of the same form as (32); in analogy with (7), we easily obtain the estimate (14) for the width  $\tilde{\eta}_{\text{int}}$  of the distribution  $N_\omega$  at  $\gamma_{\text{imp}} \ll \gamma$ .

Taking into account the approximate character of (51), we cannot draw any definite conclusions concerning the form of the line  $N_\omega$ ; one might think that it is close to the "standard form"  $N \propto \cosh^{-1}(\omega/\eta)$ . This line shape should be observed at  $\tilde{\eta}_{\text{int}} > \tilde{\eta}_T$ , i.e., at  $P > P_2$ , where  $P_2$  is given by formula (13). The quantity  $P_2$  separates the region of small supercriticality, where the broadening of the spectrum  $N_\omega$  is determined by the thermal fluctuations and the line has a Lorentz shape, from the intermediate supercriticality region, where the broadening is produced by the interaction and increases additionally because of the scattering by the defects.

4. *Region of large supercriticality.* It is characterized by the fact that the widths  $\Delta\theta$  and  $\Delta\omega$  of the distribution  $n_{\theta\omega}$  are determined only by the interaction of the waves, while the scattering by defects can in general be neglected. In this region we can retain in (43) only the last term,  $\propto T^2 N^3$ . The obtained equation has a singular solution

$$n_{\theta\omega} = N \delta(\theta - \pi/2) \delta(\omega - \omega_p/2),$$

in which  $\eta = \tilde{\eta}_{\text{int}}$  is determined by formula (15). In addition, this equation has solutions that are singular only in  $\omega$  or only in  $\theta$ , as well as a solution that is regular in both variables and apparently realized in experiments on YIG.

We were unable to obtain explicitly the regular solution, although its most interesting properties can be pointed out. The effective widths  $\Delta\theta$  and  $\Delta\omega$  of this solution are determined by the quantity  $\tilde{\eta}_{\text{int}}$  in accord with (15). It is also possible to find the asymptotic forms of this solution at

$$x = \left| \theta - \frac{\pi}{2} \right| \left( \frac{\gamma}{\eta_{\text{int}}} \right)^{1/2} \gg 1, \quad y = \left( \omega - \frac{\omega_p}{2} \right) \frac{1}{\eta_{\text{int}}} \gg 1,$$

namely

$$n_{\theta\omega} = N (\gamma/\eta_{\text{int}})^{1/2} f(x, y) \exp\{-[(\lambda_1 x)^2 + (\lambda_2 y)^2]^{1/2}\}, \quad (52)$$

where  $\lambda_1$  and  $\lambda_2 \approx 1$ , while the form of the function  $f(x, y)$  depends on the ratio of  $x$  and  $y$ :

$$f=1 \text{ at } x \ll y, \quad f \approx (y/x)^{1/2} \text{ at } y^2 > x > y, \\ f \approx 1/x^{1/2} \text{ at } x > y^2.$$

We present an interpolation formula that describes qualitatively the behavior of  $n_{\theta\omega}$  in the entire range of variation of the parameters:

$$n_{\theta\omega} \approx N (\gamma/\eta_{\text{int}})^{1/2} (1+x^2+y^2)^{1/4} \times (1+x^2+y^2)^{-3/2} \text{ch}^{-1}[(x\lambda_1)^2 + (\lambda_2 y)^2]^{1/2}. \quad (53)$$

Our experiment determines only the distribution in



frequency:

$$N_s = 2\pi \int n_{s0} d \cos \theta;$$

at  $y \gg 1$  the main contribution to this integral is made by the region  $\pi \lesssim \sqrt{y}$ , therefore

$$N_s \approx \frac{N}{\eta_{int}^2} [(\Delta\omega)^2 + \eta_{int}^2]^{1/2} \text{ch}^{-1} \frac{\Delta\omega}{\eta}. \quad (54)$$

Comparing the widths  $\eta_{int}$  (14) and  $\bar{\eta}_{int}$  (15) we can obtain an estimate (13) for the supercriticality  $P_3$ , which separates the regions of the intermediate and large supercriticality. At  $\gamma_{imp} \approx \gamma$  we have  $P_3 \approx (kv/\gamma)^{1/2}$ , which coincides with the limiting supercriticality  $P_s$  (8), up to which the vertex renormalization can be neglected.

## 5. DISCUSSION OF THE RESULTS

We have already noted, in the exposition of the experimental results, that the PSW spectral-density line shape agrees well qualitatively with the theoretical relation. We now compare quantitatively the experimental and theoretical results. Figures 4 and 5 show the results of the numerical calculation in the form of dashed lines. Taking into account the approximate character of the theory, its agreement with the experiment should be admitted to be perfectly satisfactory. A noticeable deviation of the width of the spectral density of the radiation in a polycrystal from the experimental value (see Fig. 5) can be attributed to the increase of  $\gamma_{imp}$  (it was assumed in the calculations that  $\gamma_{imp}/\gamma \approx 10^{-1}$ ). Agreement between theory and experiment for polycrystalline samples can be obtained by assuming  $\gamma_{imp} \approx \gamma$ , which agrees fully with the published data.<sup>[13]</sup>

The situation is much worse with the dependence of the width of the spectral density of the spin waves on the supercriticality, which is shown in Fig. 6. Satisfactory agreement between theory and experiment is obtained here only at low supercriticality:  $P \lesssim 1$  dB. At  $P \lesssim 5$  dB the experimental data is already only half the theoretical, and with increasing supercriticality the difference increases ever more. It can be assumed that this is due to the heating of the sample, which is acted upon by powerful continuous pumping. It is possible, how-

ever, that factors unaccounted for in the theory exist and lead to a narrowing of the PSW spectral density at large supercriticalities.

As to fluctuations of the square of the amplitude of the electromagnetic radiation from a ferrite, shown in Fig. 7, their character is in full agreement with the theory. In fact, using the correlation function  $K_B$  (18), we can show that  $\Delta B^2/\bar{B}^2 \sim 1$ , i.e., the magnitude of the fluctuations of the square of the amplitude of the electromagnetic radiation is of the order of unity, as is indeed the case in experiment (see Fig. 7).

The presented facts give grounds for assuming that the developed theory describes correctly the parametric excitation of waves in media with a nondecaying dispersion law, and all the conclusion made on its basis in various parts of the present paper (mainly in the Introduction) are perfectly well founded.

<sup>1</sup>E. R. Peressini, T. S. Hartwick, and M. T. Wess, *J. Appl. Phys.* **33**, 3292 (1962).

<sup>2</sup>F. Arams, M. Grace, and S. Okwit, *Proc. IRE* **49**, 1308 (1961).

<sup>3</sup>V. E. Sakharov, V. S. L'vov, and S. S. Starobinets, *Usp. Fiz. Nauk* **114**, 609 (1974) [*Sov. Phys. Usp.* **17**, 896 (1975)].

<sup>4</sup>V. S. L'vov, *Zh. Eksp. Teor. Fiz.* **69**, 2079 (1975) [*Sov. Phys. JETP* **42**, 1057 (1975)].

<sup>5</sup>J. E. Carroll, *Hot Electron Microwave Generators*, Am. Elsevier, 1970.

<sup>6</sup>N. N. Kiryukhin and Ya. A. Monosov, *Fiz. Tverd. Tela (Leningrad)* **13**, 1944 (1971) [*Sov. Phys. Solid State* **13**, 1631 (1972)].

<sup>7</sup>N. G. Kutovoi and G. A. Melkov, *Fiz. Tverd. Tela (Leningrad)* **17**, 958 (1975) [*Sov. Phys. Solid State* **17**, 618 (1975)].

<sup>8</sup>S. M. Rytov, *Vvedenie v statisticheskuyu radiofiziku (Introduction to Statistical Radiophysics)*, Nauka, 1976.

<sup>9</sup>R. W. Damon and H. Vande Vaart, *J. Appl. Phys.* **37**, 2445 (1966).

<sup>10</sup>V. E. Zakharov and V. S. L'vov, *Izv. Vyssh. Uchebn. Zaved. Radiofiz.* **18**, 10 (1975).

<sup>11</sup>H. W. Wyld, *Ann. Phys. (N.Y.)* **14**, 143 (1961).

<sup>12</sup>V. E. Zakharov and V. S. L'vov, *Fiz. Tverd. Tela (Leningrad)* **14**, 2913 (1972) [*Sov. Phys. Solid State* **14**, 2513 (1973)].

<sup>13</sup>G. A. Melkov, *Author's Abstract of Dissertation Physicotech. Inst. of Low Temp., Ukr. Acad. Sci., Khar'kov, 1977.*

Translated by J. G. Adashko